Inorg. Chem. **2008**, *47*, 10407−10418

Structural and Photophysical Characterization of Multichromophoric Pyridylporphyrin-Rhenium(I) Conjugates

Massimo Casanova,[†] Ennio Zangrando,[†] Elisabetta Iengo,[†] Enzo Alessio,*[,†] Maria Teresa Indelli,*[,‡] Franco Scandola,[‡] and Michele Orlandi[‡]

Dipartimento di Scienze Chimiche, University of Trieste, Via L. Giorgieri 1, 34127 Trieste, Italy, and Dipartimento di Chimica, Università di Ferrara, and INSTM, Sezione di Ferrara, 44100 Ferrara, Italy

Received May 28, 2008

Four porphyrin-Re(I) conjugates, in which a pyridylporphyrin chromophore is directly coordinated to the electron-acceptor fragment [*fac*-$Re(CO)_3(bipy)]^+$, were prepared: the dimeric and pentameric compounds [*fac*-$Re(CO)_3(bipy)(4'MPyP)](CF_3SO_3)$ (**1**) (4′MPyP = 4′-monopyridylporphyrin) and [*fac*-$\{Re(CO)_3(bipy)\}_4(\mu$-4′TPyP)]-$(CF_3SO_3)_4$ (**2**) (4′TPyP = 4′-tetrapyridylporphyrin), and the corresponding compounds with 3′ rather than 4′ porphyrins, [*fac*-$Re(CO)_3(bipy)(3'MPyP)](CF_3SO_3)$ (**3**) and [*fac*-$\{Re(CO)_3(bipy)\}_4(\mu$-3′TPyP)]$(CF_3SO_3)_4$ (**4**). These adducts proved to be very stable in solution and were also structurally characterized in the solid state by X-ray crystallography. A detailed photophysical study was performed on the zincated adducts of the conjugates **1**−**3**, labeled **5**, **6**, and **7**, respectively. In all adducts the typical fluorescence of the zinc-porphyrin unit was reduced in intensity and lifetime by the presence of the peripheral rhenium-bipy fragment(s) (heavy-atom effect). For the dyads **5** and **7** the photoinduced charge transfer process from the zinc-porphyrin to the Re(I)-bipy unit is only slightly exoergonic. Ultrafast spectroscopy experiments showed no evidence for electron transfer quenching in the dyads as such, whereas the addition of pyridine (that binds axially to zinc and thus affects the porphyrin redox potential) led to a moderately efficient photoinduced electron transfer process. In perspective, an appropriate functionalization of the bipy ligand and/or of the porphyrin chromophore might improve the thermodynamics and, thus the efficiency, of the photoinduced electron transfer process.

Introduction

We are interested in the design and construction of metal-mediated supramolecular assemblies of porphyrins and other organic chromophores (e.g., perylene bisimide dyes) for photophysical applications. In previous years we described a number of structurally and photophysically well-characterized systems in which *meso*-4′pyridylporphyrins were peripherally decorated with, or connected through, neutral Ru(II) complexes.[1]

Other examples of pyridylporphyrins (PyPs) functionalized with ruthenium compounds, starting from the pioneering work by Shi and Anson,[2] are found in the literature. The ruthenium−porphyrin conjugates, involving mainly Ru-polypyridyl complexes[3,4] but also organometallic compounds,[5] were prepared for purposes ranging from catalysis to photophysics and photodynamic therapy. Examples of porphyrins functionalized with peripheral bipy or terpy

* To whom correspondence should be addressed. E-mail: alessi@units.it (E.A.); E-mail: idm@unife.it (M.T.I.).
† University of Trieste.
‡ Università di Ferrara.

(1) (a) Iengo, E.; Zangrando, E.; Alessio, E. *Eur. J. Inorg. Chem.* **2003**, 2371–2384. (b) Scandola, F.; Chiorboli, C.; Prodi, A.; Iengo, E.; Alessio, E. *Coord. Chem. Rev.* **2006**, *250*, 1471–1496. (c) Iengo, E.; Scandola, F.; Alessio, E. *Struct. Bonding (Berlin)* **2006**, *121*, 105–144. (d) Iengo, E.; Zangrando, E.; Alessio, E. *Acc. Chem. Res.* **2006**, *39*, 841–851.

(2) (a) Shi, C.; Anson, F. C. *J. Am. Chem. Soc.* **1991**, *113*, 9564–9570. (b) Shi, C.; Anson, F. C. *Inorg. Chem.* **1992**, *31*, 5078–5083. (c) Steiger, B.; Shi, C.; Anson, F. C. *Inorg. Chem.* **1993**, *32*, 2107–2113.

(3) (a) Araki, K.; Toma, H. E. *J. Coord. Chem.* **1993**, *30*, 9–17. (b) Araki, K.; Toma, H. E. *J. Photochem. Photobiol. A* **1994**, *83*, 245–250. (c) Toma, H. E.; Araki, K. *Coord. Chem. Rev.* **2000**, *196*, 307–329. (d) Araki, K.; Losco, P.; Engelmann, F. M.; Winnischofer, H.; Toma, H. E. *J. Photochem. Photobiol. A* **2001**, *142*, 25–30. (e) Engelmann, F. M.; Losco, P.; Winnischofer, H.; Araki, K.; Toma, H. E. *J. Porphyrins Phthalocyanines* **2002**, *6*, 33–42. (f) Nogueira, A. F.; Furtado, L. F. O.; Forminga, A. L. B.; Nakamura, M.; Araki, K.; Toma, H. E. *Inorg. Chem.* **2004**, *43*, 396–398.

(4) Kon, H.; Tsuge, K.; Imamura, T.; Sasaki, Y.; Ishizaka, S.; Kitamura, N. *Inorg. Chem.* **2006**, *45*, 6875–6883.

10.1021/ic800971e CCC: $40.75
Published on Web 10/24/2008

ligands and then connected to Ru(II) fragments were reported by several groups,[6] and in particular by Sauvage and co-workers,[7] and investigated for their catalytic and photophysical properties.

Recently, we introduced in our synthetic kit also metal fragments derived from the rhenium(I)−carbonyl precursor $[ReBr(CO)_5]$.[8] Similarly to Ru(II), Re(I) also is diamagnetic (thus allowing NMR spectroscopic characterization) and makes strong and inert bonds with the pyridyl moieties of PyPs. Hupp and co-workers have described several multiporphyrin assemblies connected through the neutral *cis* bis-acceptor fragment [*fac*-$ReCl(CO)_3$].[9] We became interested to polypyridine-Re(I)-tricarbonyl complexes for their attractive electrochemical and excited-state properties: compounds containing the $[fac\text{-}Re(CO)_3(diimine)]^+$ unit are electron acceptors and display intense luminescence in the visible region in solution at ambient temperature, because of a long-lived Re → π^*(diimine) MLCT excited state, and are stable to photodecomposition.[10]

The attachment of such Re(I) fragment to other inorganic or organic chromophores for the construction of novel multichromophoric assemblies is therefore a topic of interest. In particular, for photocatalysis purposes, the ideal system should contain a photoactive unit capable of absorbing light in the visible region and subsequently transfer an electron form its excited-state to the Re(I) fragment, making it a powerful reducing agent capable of performing a rapid reduction of the substrate (e.g., CO_2). The catalytic cycle should be closed by a sacrificial electron donor. With this aim, multinuclear compounds in which $[fac\text{-}Re(CO)_3(bipy)]^+$ units are bound to Ru(II)-polypyridyl or to dirhodium(II) scaffolds have been investigated.[11,12] The connection of

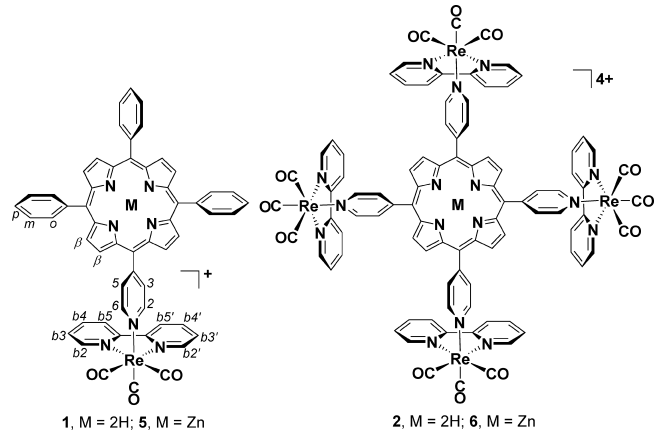

Figure 1. Schematic representation of the cations of [*fac*-$Re(CO)_3(bipy)(M\cdot4'MPyP)](CF_3SO_3)$ (**1**, M = 2H; **5**, M = Zn) with atom labeling scheme for NMR purposes and [*fac*-$\{Re(CO)_3(bipy)\}_4(\mu\text{-}M\cdot4'TPyP)](CF_3SO_3)_4$ (**2**, M = 2H; **6**, M = Zn).

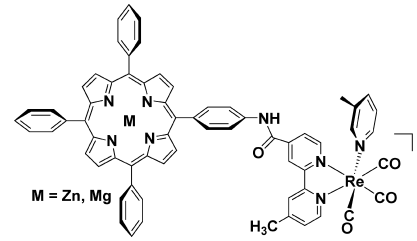

Figure 2. Schematic representation of [*fac*-$Re(CO)_3$(3-pic)(bipy-M·porph)]$^+$.[13,14]

organic chromophores, such as porphyrins, to [*fac*-$Re(CO)_3(diimine)]^+$ fragments is expected to afford systems with similar photophysical properties.[13,14]

There are basically two ways in which a [*fac*-$Re(CO)_3(diimine)]^+$ unit can be connected to a porphyrin: either the diimine is functionalized and then conjugated to a peripheral group on the porphyrin (in this case the coordination sphere of Re(I) must be completed by a sixth ligand, either neutral or anionic), or the porphyrin itself behaves as a ligand through a peripheral *meso* pyridyl group and is directly bound to the Re(I) center, adjacent to the coordinated diimine (Figure 1). The group of Perutz has described compounds of the first type, of general formula [*fac*-$Re(CO)_3(L)(bipy\text{-}M\cdot porph)]^n$ (L = Br^-, $n = 0$; L = picoline or THF, $n = +1$; $M^{2+} = Zn^{2+}$, Mg^{2+}), in which a *meso*-tetraarylmetalloporphyrin is linked via an amide bond to the bipy ligand (Figure 2).[13] When L = 3-picoline, a fast photoinduced electron transfer process from the metalloporphyrin to the Re(I)-bipy fragment was revealed by time-resolved infrared spectroscopy.[14] An evolution of this system, a triad in which a central porphyrin is bound to a $ReCl(CO)_3$ fragment and to a $[Ru(bipy)_2]^{2+}$ unit through two peripheral

(5) Schmitt, F.; Govindaswamy, P.; Süss-Fink, G.; Ang, W. H.; Dyson, P. J.; Juillerat-Jeanneret, L.; Therrien, B. *J. Med. Chem.* **2008**, *51*, 1811–1816.
(6) (a) Allwood, J. L.; Burrell, A. K.; Officer, D. L.; Scott, S. M.; Wild, K. Y.; Gordon, K. C. *Chem. Commun.* **2000**, 747–748. (b) Elliot, C. M.; Dunkle, J. R.; Paulson, S. C. *Langmuir* **2005**, *21*, 8605–8608. (c) Cho, T. J.; Shreiner, C. D.; Hwang, S.-H.; Moorefield, C. N.; Courneya, B.; Godinez, L. A.; Manriquez, J.; Jeong, K.-U.; Cheng, S. Z. D.; Newkome, G. R. *Chem. Commun.* **2007**, 4456–4458.
(7) (a) Collin, J.-P.; Heitz, V.; Sauvage, J.-P. *Tetrahedron Lett.* **1991**, *32*, 5977–5980. (b) Collin, J.-P.; Harriman, A.; Heitz, V.; Odobel, F.; Sauvage, J.-P. *J. Am. Chem. Soc.* **1994**, *116*, 5679–5690. (c) Harriman, A.; Odobel, F.; Sauvage, J.-P. *J. Am. Chem. Soc.* **1995**, *117*, 9461–9472. (d) Collin, J.-P.; Dalbavie, J.-O.; Heitz, V.; Sauvage, J.-P.; Flamigni, L.; Armaroli, N.; Balzani, V.; Barigelletti, F.; Montanari, I. *Bull. Soc. Chim. Fr.* **1996**, *133*, 749–754. (e) Flamigni, L.; Armaroli, N.; Barigelletti, F.; Balzani, V.; Collin, J.-P.; Dalbavie, J.-O.; Heitz, V.; Sauvage, J.-P. *J. Phys. Chem. B* **1997**, *101*, 5936–5943. (f) Flamigni, L.; Barigelletti, F.; Armaroli, N.; Collin, J.-P.; Sauvage, J.-P.; Williams, J. A. G. *Chem.-Eur. J.* **1998**, *4*, 1744–1754.
(8) Casanova, M.; Zangrando, E.; Munini, F.; Iengo, E.; Alessio, E. *Dalton Trans.* **2006**, 5033–5045.
(9) (a) Slone, R. V.; Hupp, J. T. *Inorg. Chem.* **1997**, *36*, 5422–5423. (b) Splan, K. E.; Keefe, M. H.; Massari, A. M.; Walters, K. A.; Hupp, J. T. *Inorg. Chem.* **2002**, *41*, 619–621. (c) Benkstein, K. D.; Stern, C. L.; Splan, K. E.; Johnson, R. C.; Walters, K. A.; Vanhelmont, F. W. M.; Hupp, J. T. *Eur. J. Inorg. Chem.* **2002**, 2818–2822. (d) Splan, K. E.; Stern, C. L.; Hupp, J. T. *Inorg. Chim. Acta* **2004**, *357*, 4005–4014. (e) Hupp, J. T. *Struct. Bonding (Berlin)* **2006**, *121*, 145–165.
(10) (a) Striplin, D. R.; Crosby, G. A. *Coord. Chem. Rev.* **2001**, *211*, 163–175. (b) Kirgan, R. A.; Sullivan, B. P.; Rillema, D. P. *Top. Curr. Chem.* **2007**, *281*, 45–100.
(11) (a) Gholamkhass, B.; Mametsuka, H.; Koika, K.; Tanabe, T.; Furue, M.; Ishitani, O. *Inorg. Chem.* **2005**, *44*, 2326–2336. (b) Sato, S.; Koike, K.; Inoue, H.; Ishitani, O. *Photochem. Photobiol. Sci.* **2007**, 454–461.
(12) Chartrand, D.; Hanan, G. S. *Chem. Commun.* **2008**, 727–729.
(13) (a) Aspley, C. J.; Lindsay Smith, J. R.; Perutz, R. N. *J. Chem. Soc., Dalton Trans.* **1999**, 2269–2271. (b) Gabrielsson, A.; Hartl, F.; Lindsay Smith, J. R.; Perutz, R. N. *Chem. Commun.* **2002**, 950–951.
(14) Gabrielsson, A.; Hartl, F.; Zhang, H.; Lindsay Smith, J. R.; Towrie, M.; Vlcek, A., Jr.; Perutz, R. N. *J. Am. Chem. Soc.* **2006**, *128*, 4253–4266.

bipy ligands in *cis* geometry was also described, but its photophysical characterization was unclear.[15]

We recently described the photophysical properties of two pyridylporphyrin-Re(I) adducts of the second type, in which a free base porphyrin is directly coordinated to the Re(I) fragment, namely, the dimeric and pentameric compounds [*fac*-Re(CO)$_3$(bipy)(4′MPyP)](CF$_3$SO$_3$) (**1**) (Figure 1, 4′MPyP = 4′-monopyridylporphyrin) and [*fac*-{Re(CO)$_3$(bipy)}$_4$(μ-4′TPyP)](CF$_3$SO$_3$)$_4$ (**2**) (Figure 1, 4'TPyP = 4′-tetrapyridylporphyrin), and briefly mentioned their preparation.[16] We found that for **1** and **2**: (i) no photoinduced electron transfer from the free-base porphyrin to the Re(I)-bipy fragment occurs for thermodynamic reasons ($\Delta G > 0$); (ii) upon excitation of the porphyrin chromophore the typical fluorescence emission is quenched because of enhanced intersystem crossing induced by the peripheral Re atoms; (iii) excitation of the Re fragments is followed by partial sensitization of the porphyrin fluorescence, indicating the occurrence of fast intercomponent energy and/or electron transfer processes.[16]

Here we describe in detail the X-ray structural characterization of **1** and **2** and of the corresponding dimeric and pentameric compounds obtained with 3′ rather than 4′ porphyrins: [*fac*-Re(CO)$_3$(bipy)(3′MPyP)](CF$_3$SO$_3$) (**3**) and [*fac*-{Re(CO)$_3$(bipy)}$_4$(μ-3′TPyP)](CF$_3$SO$_3$)$_4$ (**4**).

A detailed photophysical investigation of the three zincated derivatives [*fac*-Re(CO)$_3$(bipy)(Zn·4′MPyP)](CF$_3$SO$_3$) (**5**), [*fac*-{Re(CO)$_3$(bipy)}$_4$(μ-Zn·4′TPyP)](CF$_3$SO$_3$)$_4$ (**6**), and [*fac*-Re(CO)$_3$(bipy)(Zn·3′MPyP)](CF$_3$SO$_3$) (**7**) was performed with the aim of establishing: (i) *how* the photophysical properties of the porphyrin-Re(I) conjugates are affected by insertion of Zn into the porphyrin core: it is known that zincated porphyrins are better electron donors in their excited-state compared to the corresponding free bases, thus photoinduced electron transfer from the zinc-chromophore to the Re fragment might become allowed; (ii) *if* the number of Re(bipy) fragments and their relative geometry with respect to the porphyrin (i.e., 3′PyPs vs 4′PyPs) have an influence on the photophysical properties of the adducts; (iii) *how* the photoinduced electron transfer process might be improved (provided that it occurs), for example, by axial coordination of ligands to the Zn atom inside the porphyrin. The photophysical behavior of the zincated pentad [*fac*-{Re(CO)$_3$(bipy)}$_4$(μ-Zn·3′TPyP)](CF$_3$SO$_3$)$_4$ (**8**) was not investigated for reasons that will be discussed below.

Experimental Section

Materials. 4′PyPs and 3′PyPs were synthesized and purified as described in the literature.[17,18] The synthesis of the Re(I) precursor [*fac*-Re(CO)$_3$(bipy)(dmso-O)](CF$_3$SO$_3$) (**9**) and of the mono- and tetra-substituted 4′PyP derivatives, [*fac*-Re(CO)$_3$(bipy)-(4′MPyP)](CF$_3$SO$_3$) (**1**) and [*fac*-{Re(CO)$_3$(bipy)}$_4$(μ-4′TPyP)]-(CF$_3$SO$_3$)$_4$ (**2**), were described previously.[8,16] Chemicals were purchased from Aldrich.

Although some of the elemental analysis values, especially for C, differ from calculated values by >0.5% (most likely because of different amounts of crystallization solvent), the proposed formulas for **3**, **4**, and for all the zincated adducts are consistent with the ^{1}H NMR, and X-ray crystallographic analysis (for selected compounds).

Instrumental Methods

Unless differently stated, ^{1}H NMR spectra were collected at room temperature at 400 MHz on a Jeol Eclipse 400 FT spectrometer, with residual nondeuterated solvent signal as reference for CD_3NO_2 ($\delta = 4.33$) and $CDCl_3$ ($\delta = 7.26$) spectra. Infrared spectra (KBr) were recorded on a Perkin-Elmer 983G spectrometer or on a Perkin-Elmer 2000 NIR FT-Raman spectrometer. Elemental analysis was performed at the Dipartimento di Scienze Chimiche, University of Trieste.

UV−vis absorption spectra were recorded with a Perkin-Elmer Lambda 40 spectrophotometer. Emission spectra were taken on a Spex Fluoromax-2 spectrofluorimeter, equipped with Hamamatsu R3896 tubes.

Cyclic voltammetric measurements were carried out with a PC-interfaced Eco Chemie Autolab/Pgstat30 Potentiostat. Argon-purged 10^{-4} M sample solutions in CH_2Cl_2 (Romil, Hi-dry), containing 0.1 M [TBA]PF6 (Fluka, electrochemical grade, 99%; dried in an oven), were used. A conventional three-electrode cell assembly was used: reference electrode, a saturated calomel electrode (SCE, L 6 mm, Amel), and a platinum wire, both separated from test solution by a frit, were used as reference and counter electrodes, respectively; a glassy carbon electrode was used as a working electrode. The scan rate was 200 mV/s.

Nanosecond emission lifetimes were measured using a TCSPC apparatus (PicoQuant Picoharp300) equipped with subnanosecond LED sources (280−600 nm range, 500−700 ps pulsewidth) powered with a PicoQuant PDL 800-B variable (2.5−40 MHz) pulsed power supply. The decays were analyzed by means of PicoQuant FluoFit Global Fluorescence Decay Analysis Software.

Nanosecond transient measurements were performed with an Applied Photophysics laser flash photolysis apparatus, with frequency doubled, (532 nm, 330 mJ) or tripled, (355 nm, 160 mJ) Surelite Continuum II Nd/YAG laser (half-width 6−8 ns), Photomultiplier (Hamamatsu R928) signals were processed by means of a LeCroy 9360 (600 MHz, 5 Gs/s) digital oscilloscope.[19] Transient spectra were recorded by using as detection system a Princeton Instruments gated intensified CCD-Camera PI-MAX II equipped with an Acton SpectraPro 2300i triple grating flat field monochromator, a RB GenII intensifier, an ST133 controller and a PTG pulser.

Femtosecond time-resolved experiments were performed using a pump−probe setup based on the Spectra-Physics Hurricane Ti:sapphire laser source and the Ultrafast Systems Helios spectrometer.[19] The 560 nm pump pulses were

(15) Liu, X.; Liu, J.; Pan, J.; Chen, R.; Na, Y.; Gao, W.; Sun, L. *Tetrahedron* **2006**, *62*, 3674–3680.
(16) Ghirotti, M.; Chiorboli, C.; Indelli, M. T.; Scandola, F.; Casanova, M.; Iengo, E.; Alessio, E. *Inorg. Chim. Acta* **2007**, *360*, 1121–1130.
(17) Alessio, E.; Macchi, M.; Heath, S. L.; Marzilli, L. G. *Inorg. Chem.* **1997**, *36*, 5614–5623.
(18) Sugata, S.; Yamanouchi, S.; Matsushima, Y. *Chem. Pharm. Bull.* **1977**, *25*, 884–889.
(19) Chiorboli, C.; Rodgers, M. A. J.; Scandola, F. *J. Am. Chem. Soc.* **2003**, *125*, 483–491.

Table 1. Crystallographic Data and Details of Structure Refinements for the Free Base Compounds **1**−**4**

	1·3(CH_2Cl_2)	**2**	**3**	**4**·6(C_3H_6O)
empirical formula	$C_{60}H_{43}Cl_6N_7F_3O_6ReS$	$C_{96}H_{58}N_{16}F_{12}O_{24}Re_4S_4$	$C_{57}H_{37}N_7F_3O_6ReS$	$C_{114}H_{94}N_{16}F_{12}O_{30}Re_4S_4$
formula weight	1445.97	2920.62	1191.20	3269.09
temperature (K)	200(2)	173(2)	298(2)	100(2)
wavelength (Å)	1.54178	1.54178	0.71073	1.0000
crystal system	triclinic	orthorhombic	monoclinic	monoclinic
space group	$P\bar{1}$	$P2_12_12_1$	$P2_1/c$	$P2_1/c$
a (Å)	10.566(3)	16.546(4)	24.461(4)	20.479(4)
b (Å)	12.476(3)	19.760(5)	13.716(3)	15.689(3)
c (Å)	24.170(5)	39.363(6)	17.318(4)	22.865(4)
α (°)	102.09(3)			
β (°)	91.37(3)		105.56(3)	108.733(14)
γ (°)	100.27(2)			
volume (Å^3)	3059.3(13)	12870(5)	5597(2)	6957(2)
Z	2	4	4	2
D_{calcd} (g cm^{-3})	1.570	1.507	1.414	1.561
μ Mo Kα, (mm^{-1})	7.162	8.497	2.272	−
F(000)	1440	5640	2376	3204
θ_{max} (°)	67.49	63.37	23.36	30.17
reflns collected	39858	92363	33997	36421
unique reflections	9543	17392	7689	6815
R_{int}	0.0870	0.0880	0.0705	0.0406
observed $I > 2\sigma(I)$	6828	9959	3430	5450
parameters	757	1369	676	811
goodness of fit	1.134	1.006	0.732	1.037
$R1$ ($I > 2\sigma(I)$)[a]	0.1263	0.0858	0.0380	0.0310
$wR2$[a]	0.3154	0.2245	0.0776	0.0760
$\Delta\rho$ (e/Å^3)	2.445, −1.939[b]	1.599, −1.231[b]	0.360, −0.668	0.591, −0.735

[a] $R1 = \Sigma \; ||Fo| - |Fc||/\Sigma|Fo|$, $wR2 = [\Sigma \; w(Fo^2 - Fc^2)^2/\Sigma w(Fo^2)^2 \;]^{1/2}$. [b] Residual peak at ca. 1.2 Å from Re ions.

generated with a Spectra Physics 800 OPA. Probe pulses were obtained by continuum generation on a sapphire plate (useful spectral range, 450−800 nm). Effective time resolution ca. 300 fs, temporal chirp over the white-light 450−750 nm range ca. 200 fs, temporal window of the optical delay stage 0−1000 ps. The time-resolved spectral data were analyzed with the Ultrafast Systems Surface Explorer Pro software.

All the photophysical experiments refer to dilute solutions (concentrations in the range $2-8 \times 10^{-5}$ M) in dichloromethane. The time-resolved absorption experiments were carried out in dichloromethane solutions saturated with potassium carbonate, to remove traces of acidity that were found to promote photodecomposition under prolonged laser irradiation.[16]

Crystallographic Measurements. Crystals of the free-base porphyrin-Re(I) conjugates suitable for X-ray diffraction were obtained by diffusion of diethyl ether into dichloromethane (**1**, **2**) or acetone (**3**, **4**) solutions. Crystal data and details of data collections and refinements for the structures reported are summarized in Table 1. Data collections for **1**, **2**, and **3** were carried out on a Cu rotating anode ($\lambda = 1.54178$ Å), graphite monochromatized, equipped with a Brucker CCD2000 detector. Data collection for **4** was performed at the X-ray diffraction beamline at Synchrotron Elettra, Trieste (Italy), using a monochromatized wavelength of 1.0000 Å. Cell refinement, indexing and scaling of all the data sets were performed using the programs Denzo and Scalepack.[20] All the structures were solved by direct methods and subsequent Fourier analyses and refined by the full-matrix least-squares method based on F^2 with all observed reflections.[21] Besides the triflate counteranions, the difference Fourier maps revealed in the asymmetric unit the presence of three CH_2Cl_2 molecules in **1** and of three independent acetone molecules in **4**. The contribution of hydrogen atoms at calculated positions were included in final cycles of refinement. All the calculations were performed using the WinGX System, Ver 1.64.[22]

Syntheses. [*fac*-Re(CO)$_3$(bipy)(3′MPyP)](CF$_3$SO$_3$) (3). 3′MPyP (57 mg, 9.23×10^{-2} mmol) was dissolved in 20 mL of an acetone/dichloromethane (1:1) mixture. After addition of 50 mg (7.64×10^{-2} mmol) of [*fac*-Re(CO)$_3$(bipy)-(dmso-O)](CF$_3$SO$_3$) (**9**) the mixture was heated to reflux for 20 h and then concentrated in vacuo to ca. 5 mL, after filtration on fine paper for removing unreacted 3′MPyP. Purple microcrystals of the product formed upon addition of a few drops of diethyl ether until saturation, and were removed by filtration, washed with diethyl ether and vacuum-dried. Yield: 80 mg (88%). Found; C, 56.8; H, 3.05; N, 8.10. $C_{57}H_{37}N_7F_3O_6ReS$ ($M_W = 1191.21$) requires C, 57,4; H, 3.13, N, 8.23. ^{1}H NMR (δ, $CDCl_3$, see Figure 8 for labeling scheme): 9.12 (s, 1H, H2); 9.08 (d, 2H, b6,6′); 9.06 (d, 2H, b3,3′); 8.88 (m, 6H, βH); 8.69 (d, 1H, H6); 8.45 (d, 1H, H4); 8.39 (t, 2H, b4,4′); 8.30 (d, 2H, βH); 8.22 (m, 6H, *o*H); 7.80 (m, 10H, H5 + *m* + *p*H); 7.62 (t, 2H, b5,5′). Selected IR (KBr, cm^{-1}): νCO 2030 (s) 1930 and 1919 (s, br).

[*fac*-{Re(CO)$_3$(bipy)}$_4$(μ-3′TPyP)](CF$_3$SO$_3$)$_4$ (4). 3′TPyP (5.7 mg, 9.16×10^{-3} mmol) was dissolved in 20 mL of an acetone/dichloromethane (1:1) mixture. After addition of 30 mg (4.5×10^{-2} mmol) of **9** the mixture was heated to reflux for 24 h and then concentrated in vacuo to ca. 5 mL, after filtration on fine paper for removing unreacted 3′TPyP.

(20) Otwinowski, Z.; Minor, W. In Processing of X-ray Diffraction Data Collected in Oscillation Mode; Carter, C. W., Jr., Sweet, R. M., Eds.; *Methods in Enzymology, Macromolecular Crystallography Part A*; Academic Press: New York, 1997; Vol. *276*, pp 307−326.
(21) Sheldrick, G. M. *SHELX97, Programs for Crystal Structure Analysis (Release 97-2)*; University of Göttingen: Göttingen, Germany, 1998.
(22) Farrugia, L. J. *J. Appl. Crystallogr.* **1999**, *32*, 837–838.

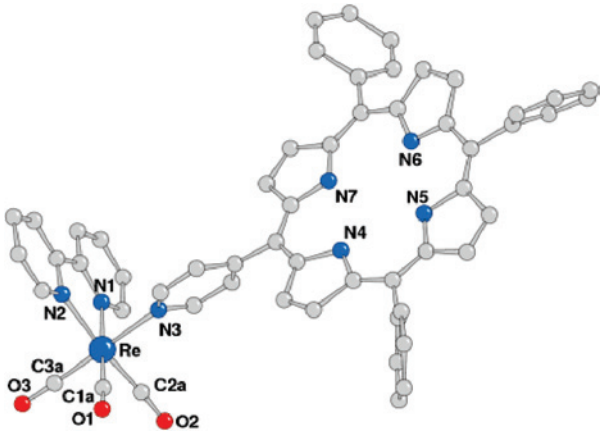

Figure 3. Molecular structure of the complex cation of **1** with selected atom labeling scheme.

Purple microcrystals of the product formed upon addition of a few drops of diethyl ether until saturation and were removed by filtration, washed with diethyl ether and vacuum-dried. Yield: 16 mg (60%). Found (for crystals): C, 41.2; H, 2.82; N, 6.70. $C_{96}H_{58}N_{16}F_{12}O_{24}Re_4S_4 \cdot 6(CH_3COCH_3)$ (M_W = 3269.09) requires C, 41.9; H, 2.90; N, 6.85. ^{1}H NMR (δ, CD_3NO_2) see text. Selected IR (KBr, cm^{-1}): νCO 2030 (s) 1929 and 1920 (s, br).

Zincated Adducts. Insertion of zinc into the free-base pyridylporphyrin-Re(I) conjugates was performed according to this general procedure: a concentrated CH_2Cl_2 solution of each compound was treated overnight with an 8-fold molar excess of $Zn(CH_3COO)_2$ dissolved in the minimum amount of MeOH. The solution was dried in vacuo and the obtained solid dissolved in CH_2Cl_2.The product was precipitated by addition of *n*-hexane, removed by filtration, washed thoroughly with cold methanol and diethyl ether and vacuum-dried. Yield > 85%. The compounds were characterized by UV−vis and ^{1}H NMR spectroscopy.

[*fac*-Re(CO)$_3$(bipy)(Zn·4′MPyP)](CF$_3$SO$_3$) (5). ^{1}H NMR (δ, $CDCl_3$ + CD_3OD, see Figure 1 for labeling scheme): 9.27 (d, 2H, b6,6′); 9.00 (d, 2H, b3,3′); 8.96 (d, 2H, βH); 8.92 (m, 4H, βH); 8.63 (d, 2H, βH); 8.51 (d, 2H, H2,6); 8.42 (t, 2H, b4,4′); 8.18 (m, 8H, H3,5 + *o*H); 7.82 (t, 2H, b5,5′); 7.74 (m, 9H, *m* + *p*H).

[*fac*-{Re(CO)$_3$(bipy)}$_4$(μ-Zn·4′TPyP)](CF$_3$SO$_3$)$_4$ (6). ^{1}H NMR (δ, CD_3OD, see Figure 1 for labeling scheme) 9.52 (d, 8H, b6,6′), 8.81 (d, 8H, H2,6), 8.79 (d, 8H, b3,3′), 8.63 (s, 8H, βH), 8.47 (t, 8H, b4,4′), 8.11 (d, 8H, H3,5), 7.98 (t, 8H, b5,5′).

[*fac*-Re(CO)$_3$(bipy)(Zn·3′MPyP)](CF$_3$SO$_3$) (7). ^{1}H NMR (δ, $CDCl_3$ + CD_3OD, see Figure 8 for labeling scheme): 9.10 (d, 2H, b6,6′); 8.95 (s, 1H, H2); 8.88 (m, 4H, βH); 8.80 (m, 4H, b3,3′ + βH); 8.63 (d, 1H, H6); 8.49 (d, 1H, H4); 8.30 (t, 2H, b4,4′); 8.30 (d, 2H, βH); 8.18 (m, 8H, *o*H + βH); 7.73 (m, 10H, H5 + *m* + *p*H); 7.61 (t, 2H, b5,5′).

[*fac*-{Re(CO)$_3$(bipy)}$_4$(μ-Zn·3′TPyP)](CF$_3$SO$_3$)$_4$ (8). See text for ^{1}H NMR spectrum.

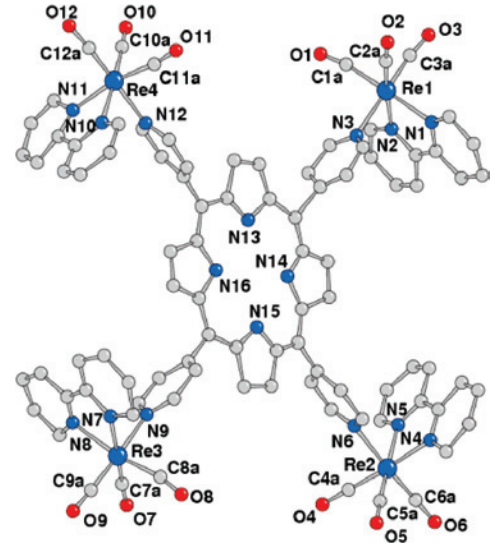

Figure 4. Molecular structure of the complex cation of **2** with selected atom labeling scheme.

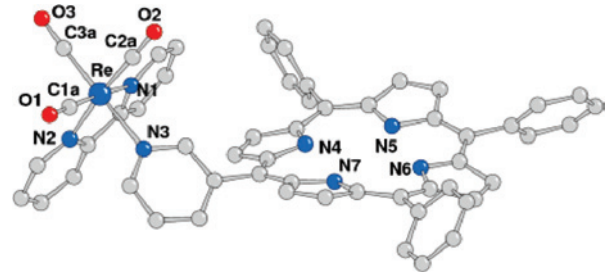

Figure 5. Molecular structure of the complex cation of **3** with selected atom labeling scheme.

Results

Preparation and Solid State Structures of the Free-Base Pyridylporphyrin-Re(I) Conjugates 1−4. We showed that [*fac*-Re(CO)$_3$(bipy)(dmso-O)](CF$_3$SO$_3$) (**9**) is a good precursor for the efficient preparation of luminescent [*fac*-Re(CO)$_3$(bipy)(L)](CF$_3$SO$_3$) complexes by replacement of the weakly bound dmso-O with an N-donor heterocycle (L).[8] Treatment of either 4′MPyP or 4′TPyP with a slight excess of **9** afforded the mono- and tetra-substituted porphyrins, [*fac*-Re(CO)$_3$(bipy)(4′MPyP)](CF$_3$SO$_3$) (**1**) and [*fac*-{Re(CO)$_3$(bipy)}$_4$(μ-4′TPyP)](CF$_3$SO$_3$)$_4$ (**2**), respectively, in pure form and acceptable yields.[16] With a similar synthetic procedure we now also prepared the isomeric compounds with the corresponding 3′-pyridylporphyrins, [*fac*-Re(CO)$_3$(bipy)(3′MPyP)](CF$_3$SO$_3$) (**3**) and [*fac*-{Re(CO)$_3$(bipy)}$_4$(μ-3′TPyP)](CF$_3$SO$_3$)$_4$ (**4**), respectively.

The X-ray molecular structures of the cations of **1**, **2**, **3**, and **4** are shown in Figures 3−6, respectively. In all compounds the Re centers display a distorted octahedral coordination sphere comprising three carbonyl ligands linearly coordinated in *fac* geometry, a bipy and a pyridyl ring from the *meso*-porphyrin. The coordination bond lengths and angles (selected values are reported in Tables 2−4) are unexceptional and in agreement with those of similar Re complexes,[8] although the data of **1** and **2** are of lower accuracy.

Table 2. Selected Coordination Bond Lengths (Å) and Angles (°) for Compounds **1** and **3**

	1	**3**
Re−N(1)	2.24(3)	2.160(6)
Re−N(2)	2.22(3)	2.143(7)
Re−N(3)	2.19(2)	2.215(6)
Re−C(1a)	1.91(4)	1.840(9)
Re−C(2a)	1.97(4)	1.824(9)
Re−C(3a)	1.91(3)	1.873(9)
N(1)−Re−N(2)	74.4(11)	74.9(3)
C(1a)−Re−N(1)	174.9(12)	172.8(3)
C(2a)−Re−N(2)	171.6(13)	171.2(3)
C(3a)−Re−N(3)	176.7(11)	177.8(3)

Table 3. Selected Coordination Bond Lengths (Å) and Angles (°) for Compound **2**

Re(1)−N(1)	2.157(16)	Re(3)−N(7)	2.091(19)
Re(1)−N(2)	2.16(2)	Re(3)−N(8)	2.250(18)
Re(1)−N(3)	2.284(18)	Re(3)−N(9)	2.168(19)
Re(1)−C(1a)	1.893(15)	Re(3)−C(7a)	1.869(15)
Re(1)−C(2a)	1.890(14)	Re(3)−C(8a)	1.916(17)
Re(1)−C(3a)	1.782(19)	Re(3)−C(9a)	1.820(17)
Re(2)−N(4)	2.15(2)	Re(4)−N(10)	2.16(2)
Re(2)−N(5)	2.151(19)	Re(4)−N(11)	2.11(2)
Re(2)−N(6)	2.249(14)	Re(4)−N(12)	2.253(13)
Re(2)−C(4a)	1.896(16)	Re(4)−C(10a)	1.881(15)
Re(2)−C(5a)	1.880(14)	Re(4)−C(11a)	1.880(16)
Re(2)−C(6a)	1.788(18)	Re(4)−C(12a)	1.81(2)
N(1)−Re(1)−N(2)	73.7(7)	N(7)−Re(3)−N(8)	73.6(8)
C(1a)−Re(1)−N(1)	176.0(9)	C(7a)−Re(3)−N(7)	167.7(10)
C(2a)−Re(1)−N(2)	171.1(8)	C(9a)−Re(3)−N(9)	176.4(9)
C(3a)−Re(1)−N(3)	178.4(12)	C(8a)−Re(3)−N(8)	170.1(13)
N(4)−Re(2)−N(5)	74.3(8)	N(10)−Re(4)−N(11)	73.9(8)
C(4a)−Re(2)−N(4)	174.5(9)	C(10a)−Re(4)−N(10)	174.2(10)
C(5a)−Re(2)−N(5)	169.4(9)	C(11a)−Re(4)−N(11)	167.5(9)
C(6a)−Re(2)−N(6)	175.6(9)	C(12a)−Re(4)−N(12)	176.1(12)

The porphyrin macrocycle in both mononuclear compounds **1** and **3** presents a warped geometry, more apparent in **3** (Figure 7), and testified by the values of the dihedral angles formed by the opposite pyrrole rings in each macrocycle: 20(2), 11(2)° in **1**, and 24.0(4), 27.2(4)° in **3**. As a consequence, the best fit plane through the porphyrin shows significant displacements of atoms up to ±0.41(3) Å in **1**, and ±0.525(6) Å in **3** (Figure 7). The *meso* pyridyl and phenyl rings form dihedral angles with the best-fit plane of the porphyrin that fall in the range 50.7(9)−67.1(7)° for **1**, and 46.1(1)−67.1(2)° for **3**, most likely for optimizing the crystal packing. It is worth noting that the angle value relative

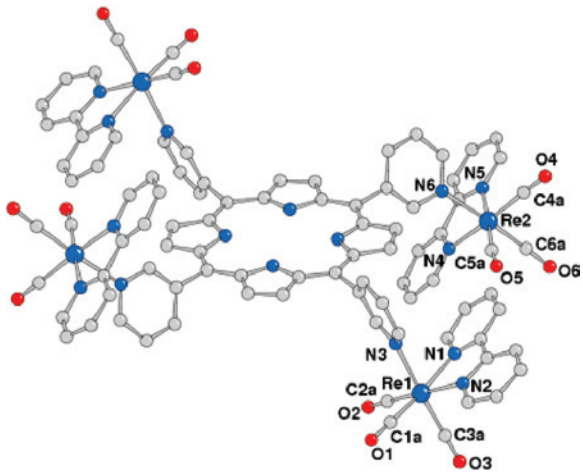

Figure 6. Molecular structure of the centrosymmetric complex cation of **4** with selected atom labeling scheme.

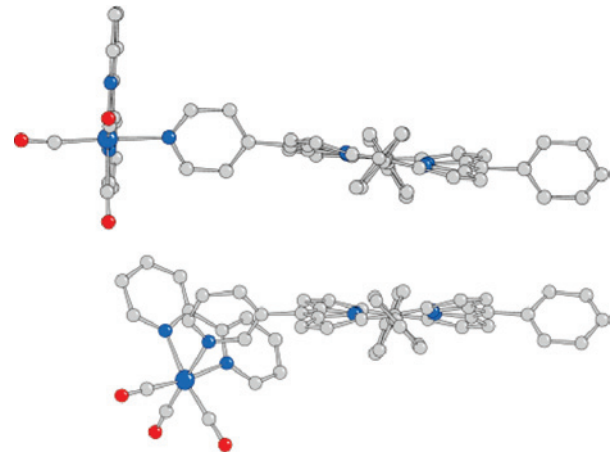

Figure 7. Side views of the complex cation of **1** (top) and **3** (bottom) that show the porphyrin ring distortions and the different distances between the porphyrin and the Re(I) fragment.

to the pyridyl ring is the largest in **1** (67.1(7)°), but rather narrow in **3** (46.1(1)°).

For obvious geometrical reasons related to the position of the pyridyl N atom, the dihedral angle between the bipy ligand and the porphyrin is close to 90° in **1** (85.9(4)°), while it is much narrower in **3** (64.6(1)°). As a consequence, in **3** a side of bipy is in close proximity to one pyrrole ring of 3′MPyP and the distance between the porphyrin centroid and Re is remarkably shorter in **3** (8.55 Å) than in **1** (9.96 Å).

The crystal packings of **1** and **3** show pairs of molecules arranged about a center of symmetry, indicating a $\pi-\pi$ interaction between the macrocycles although they are slightly offset (distance between the porphyrin centroids: 5.32 in **1** and 5.05 Å in **3**) (Supporting Information). The shortest stacking distance (calculated between the inner nitrogen atoms) is relatively small in **3** (3.67 Å) and somewhat larger in **1** (4.07 Å). The pairing of the complexes seems to be favored in **3** by the orientation assumed by the pyridyl and phenyl rings about the porphyrin (see above). On the other hand, in both complexes the peripheral aromatic rings are not involved in any significant $\pi-\pi$ interaction.

The crystal structure analysis of **2** and **4** indicate tetranuclear cations composed of four [*fac*-Re(CO)$_3$(bipy)]$^+$ units appended to the 4′TPyP and 3′TPyP macrocycles, respectively (Figures 4 and 6). In both compounds the porphyrin atoms are almost coplanar (in contrast with the deformations observed in the mononuclear complexes): the largest atom deviation from the porphyrin mean plane is ± 0.13(2) Å in **2** and ±0.061(6) Å in **4**, respectively. In **2** all Re atoms are crystallographically independent and the conformation shows an approximately D_{2h} symmetry with adjacent [Re(CO)$_3$(bipy)] fragments arranged in a pairwise fashion: bipy ligands on Re units coordinated to pyridyl rings at *meso* positions 5, 10 (and 15, 20) face each other, while those on the *meso* positions 5, 20 (and 10, 15) are far apart (Figure 4). The peripheral Re(1) and Re(3) atoms show a small, but significant, displacement from the porphyrin plane (−1.15(2) Å and +0.94(2) Å, respectively), while the corresponding values for Re(2) and Re(4) are negligible. The *meso* pyridyl rings connected to Re(1) and Re(3) are oriented almost perpendicularly with respect to the porphyrin mean plane

(89.3(5) and 83.6(5)°, respectively), while those attached to Re(2) and Re(4) form with it dihedral angles of 68.1(4) and 64.0(4)°, respectively. In **2** the potential solvent area in the unit cell accounts for 28.4% of the volume, but the low quality of the crystals did not allow us to successfully refine solvent molecules.

Complex **4** is located on a crystallographic symmetry center. In the solid state this compound has a step-like geometry, with two adjacent Re fragments above, and the other two below, the porphyrin plane (Figure 6). Thus the central 3′TPyP has a *1,2-alternate* conformation. The peripheral Re(I) ions show different displacements from the porphyrin mean plane: 4.01(1) Å for Re(1) and 2.252(8) Å for Re(2), due to the different conformations assumed by the [Re(CO)$_3$(bipy)] fragments about the C(py)−C(*meso*) bonds. The acetone solvent molecules in **4**, which are distributed in the lattice among the tetranuclear complexes and the triflate anions, do not show any unusual short contact. The presence of the [*fac*-Re(CO)$_3$(bipy)]$^+$ units about the porphyrin ring hampers any $\pi-\pi$ stacking interaction between the macrocycles.

The structural information gathered for the free-base pyridylporphyrin-Re(I) conjugates **1**−**4** can be safely transferred to the corresponding zincated adducts, subject of the photophysical investigation reported below.

^{1}H NMR Spectroscopy of the Pyridylporphyrin-Re(I) Conjugates 1−8. The ^{1}H NMR spectra of **1** and **2** in $CDCl_3$ show sharp signals exclusively, and are consistent with the solid state structures (Supporting Information). The resonances of the porphyrin and of the bipy ligands (four, consistent with the symmetry of the molecules) were assigned by means of conventional H−H COSY spectra. In the spectrum of **2** a single set of bipy signals was observed, implying that all four metal fragments are equivalent by virtue of free rotation about the Re−N(py) bonds. The doublet at $\delta = 8.83$ was unambiguously assigned to the pyridyl protons closest to the coordinated N atom (H2,6), as it shows a clear NOE effect with the resonance of the bipy protons in 6,6′ positions (most downfield resonance at $\delta = 9.51$). In general, coordination of the pyridyl ring to the [*fac*-ReX(CO)$_3$] fragment (X = Cl or Br) induces a typical downfield shift for the resonance of H2,6 protons.[9] On the contrary, in the spectra of both **1** and **2**, as in similar model complexes,[8] the H2,6 doublet is shifted *upfield* compared to the unbound porphyrin because of the shielding effect of the adjacent, and almost orthogonal, bipy ligand.

The spectrum of the monomer compound with 3′MPyP, **3** (Figure 8), is straightforward and totally consistent with the solid state structure, suggesting that a similar geometry is maintained, as an average, in solution. The resonance of H2 ($\delta = 9.12$) is the most downfield implying that, as in the solid state, the 3′-pyridyl ring is oriented in such a way that H2 points away from bipy and is not influenced by its shielding cone. Conversely, the resonance of two pyrrole protons is remarkably shifted upfield compared to the other six ($\delta = 8.28$ vs 8.86). The X-ray structure shows that the H atoms of the N4 pyrrole ring are quite close to the centroid of the bipy ring containing N1 (Figure 5): in solution the pyrrole protons adjacent to the pyridyl ring apparently remain into the shielding cone of bipy, averaged by a tilting motion of the Re fragment relative to the porphyrin (full rotation is probably hindered).

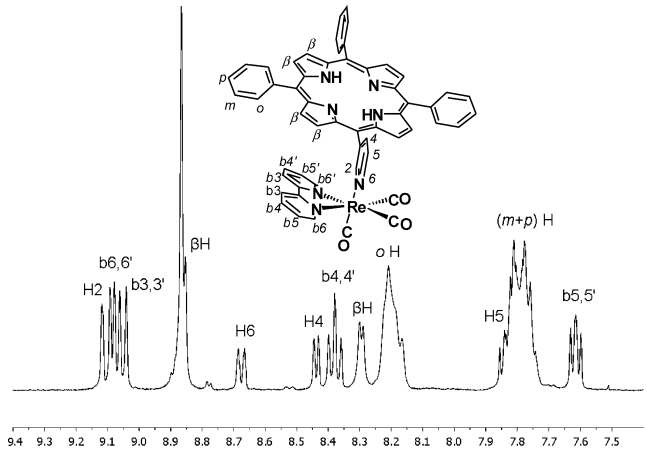

Figure 8. Downfield region of the ^{1}H NMR spectrum ($CDCl_3$, 400 MHz) of **3** with labeling scheme.

The ^{1}H NMR spectrum of **4** (crystalline material) at room temperature is quite complex. In all solvents investigated (CD_3NO_2, $CDCl_3$, CD_2Cl_2, acetone-d_6) it shows a manifold of relatively broad and overlapping multiplets (Supporting Information), suggesting the coexistence of several conformers, owing to hindered rotation about the C(*meso*)−C(pyridyl) bond (and perhaps also the N−Re bond). The effect of temperature on the NMR spectrum of **4** was investigated in acetone-d_6 (−75 °C < T < 25 °C) and in CD_3NO_2 (25 °C < T < 75 °C), but no significant improvement was obtained. Thus, no assignment was attempted.

Insertion of Zn(II) into the porphyrin core of the four porphyrin-Re(bipy) conjugates **1**−**4** was efficiently performed by treatment with excess zinc acetate in methanol/dichloromethane mixtures. The zincated adducts **5** and **6** proved to be less soluble in $CDCl_3$ or CD_2Cl_2 compared to the free-base compounds, suggesting a stronger aggregation in the solid state.[23] The 3′PyP compounds **7** and **8** maintained instead a fair solubility, even though lower than the corresponding free-base compounds. In all cases, good solubility was recovered by addition of a few microliters of CD_3OD. The ^{1}H NMR spectrum of **7** in pure $CDCl_3$ showed relatively broad and badly resolved peaks, consistent with the occurrence of aggregation also in solution. Addition of CD_3OD increased the solubility and induced the appearance of a normal spectrum, with sharp peaks, as methanol coordinates to Zn and disrupts aggregation. Anyhow, the ^{1}H NMR spectra of the zincated adducts **5**−**8** were very similar to those of the corresponding free-base compounds (Supporting Information), suggesting that the solution structures are not significantly affected by the presence of zinc inside the porphyrin core.

Photophysical Behavior of the Zincated Pyridylporphyrin-Re(I) Conjugates 5−7. The zincated tetraphenylporphyrin, Zn·TPP,[24] and the rhenium complex [*fac*-Re-

(23) Presumably for the same reason, 6 turns green (from purple) in the solid state upon drying.

Table 4. Selected Coordination Bond Lengths (Å) and Angles (°) for Compound **4**

Re(1)−N(1)	2.266(5)	Re(2)−N(4)	2.273(6)
Re(1)−N(2)	2.268(5)	Re(2)−N(5)	2.278(5)
Re(1)−N(3)	2.324(6)	Re(2)−N(6)	2.331(6)
Re(1)−C(1a)	2.010(8)	Re(2)−C(4a)	2.027(8)
Re(1)−C(2a)	2.037(9)	Re(2)−C(5a)	2.010(9)
Re(1)−C(3a)	2.003(9)	Re(2)−C(6a)	1.979(9)
N(1)−Re(1)−N(2)	75.0(2)	N(4)−Re(2)−N(5)	75.2(2)
C(1a)−Re(1)−N(1)	169.9(2)	C(4a)−Re(2)−N(4)	173.0(2)
C(2a)−Re(1)−N(2)	173.4(2)	C(5a)−Re(2)−N(5)	177.5(2)
C(3a)−Re(1)−N(3)	176.4(3)	C(6a)−Re(2)−N(6)	177.1(3)

$(CO)_3$(bipy)(py)][CF_3SO_3] (**10**),[16] were used as references. For reasons that will be illustrated below, and consistent with our previous results,[16] the energetic for the photoinduced electron transfer process is expected to be less favorable for the pentameric species with respect to the dimeric systems. Nevertheless, the pentameric adduct **7** was included in the photophysical investigation as a useful probe to discriminate between different mechanisms (see Discussion).

Absorption Spectra. The relevant absorption properties of the systems in the visible region are collected in Table 5. As observed for the corresponding free-base compounds **1** and **2**,[16] aside from small red shifts of the porphyrin bands with respect to the parent zinc-porphyrin, the spectra of **5**−**7** are good superpositions of those of the molecular components, confirming that the electronic interaction between the zinc-porphyrin and rhenium units is weak. They are dominated in the whole spectral region by the zinc-porphyrin component (Figure 9), with two typical Q-bands between 500 and 700 nm in addition to the Soret band. The rhenium unit practically does not absorb in the visible region above 350 nm. In the UV region the metal-to-ligand charge-transfer (MLCT) Re → bipy bands (λ_{max} = 350 nm) are hidden by the porphyrin Soret band, while the intense ligand centered (LC) transitions are evident under 330 nm with a narrow band at 321 nm that can be clearly recognized only in the spectrum of **6**.

Finally, the spectra were not concentration-dependent, suggesting that no aggregation occurs for these compounds in the range of concentrations used.

Emission. Emission experiments were performed upon selective excitation of zinc-porphyrin component in the Q-bands region. All the Zn·porphyrin-Re(I) conjugates studied show the typical porphyrin-based fluorescence. The emission spectrum of each compound exhibits two intense sharp bands like that of the zinc-porphyrin model, with a small red-shift with respect to the reference chromophore (see Table 6). Excitation of optically matched solutions of the dyad **5** and of the Zn·TPP reference at the excitation wavelength of 517 nm showed a moderate but significant decrease of the emission intensity and lifetime for the

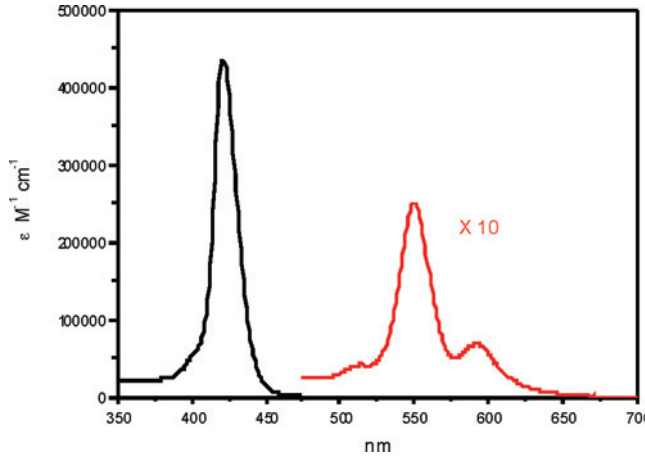

Figure 9. Absorption spectrum of [*fac*-Re(CO)$_3$(bipy)(Zn·4′MPyP)]-(CF_3SO_3) (**5**) in dichloromethane solution: Soret band (black line) and Q bands (red line).

Table 5. Absorption Maxima (λ_{max}, nm) of **5**−**7**, and of the Reference Compound Zn·TPP in CH_2Cl_2 Solution

compound	Soret	Q_1	Q_2
Zn·TPP	420	547	585
5	421	550	592
6	438	564	605
7	421	550	592

rhenium adduct. This effect is more pronounced for the pentad **6**. In conclusion, the data of Table 6 clearly indicate that, in all the adducts studied, the porphyrin fluorescence is affected, but not strongly quenched, by the presence of the peripherally bound rhenium unit(s).

In order to show effects of solvent polarity on the emission behavior, measurements (emission quantum yield and lifetime) in CH_3CN were also carried out. The results clearly showed that, for these systems, the emission properties are practically unaffected by the solvent polarity.

For **5** emission experiments were also performed in the presence of pyridine (0.5−2 M),[25] that is known to bind axially to the zinc atom.[26,27] Remarkably, the presence of pyridine induced a pronounced shortening in the lifetime of **5** (from 900 ps to ca. 250 ps), accompanied by a proportional decrease of the emission intensity, whereas it had no effect on the emission behavior (intensity and lifetime) of Zn·TPP.

Emission experiments were also carried out upon excitation in the ultraviolet region (λ = 321 nm) where the Re(I)-bipy unit absorbs. As expected on the basis of our previous results with the free base adducts,[16] no rhenium MLCT emission was detected, clearly indicating that its triplet state is efficiently quenched in all the compounds investigated. Although a detailed characterization of the photophysical

(24) Concentration-dependent self-assembly of zincated pyridylporphyrins is known to occur spontaneously in noncoordinating solvents through axial Zn−N(pyridyl) interactions (see Fleischer, E.; Shachter, A. M. *Inorg. Chem.* **1991**, *30*, 3763−3769.). Indeed, the absorption and emission spectra of Zn·4′MPyP and Zn·3′MPyP in CH_2Cl_2 solutions were found to be concentration-dependent. Reference spectra were taken for concentrations below 10^{-5} M, where no further changes were observed upon dilution. In these conditions, Zn·4′MPyP and Zn·3′MPyP showed spectral patterns and photophysical behaviors almost identical to Zn·TPP that was therefore selected as reference compound.

(25) To ascertain the stability of the compounds in the presence of pyridine, a sample of **5** was dissolved in neat pyridine-d_5, and its ^{1}H NMR spectrum was monitored in time. Only after one day, very weak signals corresponding to the resonances of free Zn·4′MPyP started to appear, indicating that the Re−PyP bond has an excellent kinetic stability.

(26) Gust, D.; Moore, T. A.; Moore, A. L.; Kang, H. K.; DeCraziano, J. M.; Liddell, P. A.; Seely, G. R. *J. Phys. Chem.* **1993**, *97*, 13637–13642.

(27) Similarly to what reported by Gust and co-workers for the Zn·TPP chromophore (ref 26), the addition of pyridine caused small but significant spectral shifts (ca. 15 nm) in the absorption (Q region) as well as in the emission spectra of the dyad **5**, clearly indicating the coordination of pyridine to the zinc center.

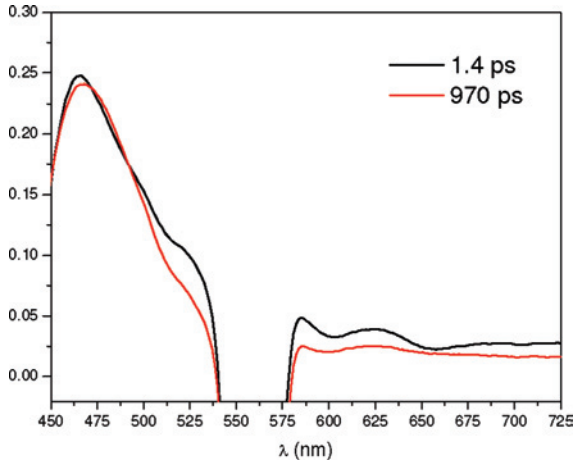

Figure 10. Transient spectral changes obtained for **5** in CH_2Cl_2 solution. Excitation wavelength: 560 nm.

behavior following excitation of the rhenium unit(s) was not attempted, given the energy level diagram of the system (see below) the quenching is likely to occur by intramolecular electron transfer.

Transient Absorption. Transient absorption spectra of **5**−**7** were measured in deaerated dichloromethane solutions by using nanosecond laser flash photolysis (532 nm laser excitation) in the spectral range 460−520 nm, where the triplet state of the Zn·porphyrin-Re(I) adducts exhibits distinct absorptions.[1b] The transient spectra were compared with that of an isoabsorptive solution of Zn·TPP. For all derivatives the transient, that decayed with a lifetime > 20 μs, corresponded to the spectrum of triplet state. The intensity of each transient was very similar to that observed for the reference compound (Supporting Information), clearly indicating that in these compounds the yield of triplet formation is the same as in Zn·TPP.

The photophysical behavior of each adduct was further investigated by ultrafast spectroscopy using 560 nm excitation. The transient spectral changes of **5** are shown in Figure 10. The initial spectrum, taken immediately after the excitation pulse (1 ps) exhibited the typical zinc-porphyrin S_1 features (a strong broad positive absorption at 460 nm, ground-state bleaching and stimulated emission in the range 590−660 nm). This pattern evolved to a final spectrum that is practically superimposable to that of the nanosecond experiments and thus corresponds to the triplet spectrum. The evolution of the S_1 spectrum to that of the triplet takes place in ca.1 ns, a time consistent with the singlet lifetime observed in the luminescence decay (see Table 6).

Ultrafast experiments were also performed in the presence of pyridine. The temporal evolution of spectral changes was substantially different from that observed in the absence of pyridine, with a biphasic behavior taking place for $t \leq 80$ ps (Figure 11a) and $t \geq 80$ ps (Figure 11b). Kinetic analysis of the spectral changes at 618 nm yielded a time constant of 20 ps for the first process (Figure 11a) and of 300 ps at 585 nm for the second process (Figure 11b). No clear evidence for the characteristic spectral features of the porphyrin radical

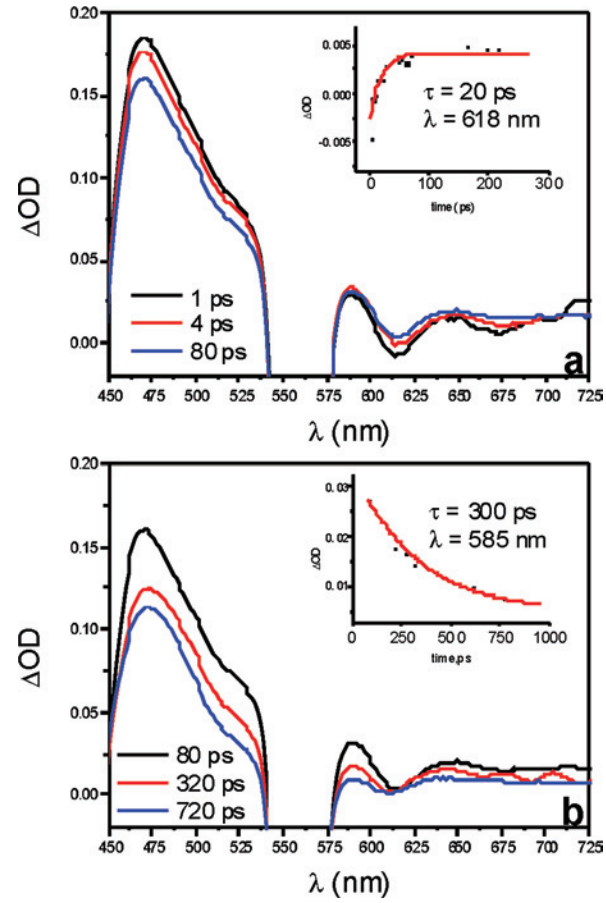

Figure 11. Transient spectral changes obtained for **5** in CH_2Cl_2 solution in the presence of pyridine (excitation wavelength: 560 nm). (a) Spectral changes in the 1−80 ps range; inset: kinetic recorded at 618 nm. (b) Spectral changes in the 80−1000 ps range; inset: kinetic recorded at 585 nm.

Table 6. Emission Properties of **5**−**7**, and of the Reference Compound Zn·TPP in CH_2Cl_2 Solution[a]

compound	λ_{max}(em), nm	Φ_0/Φ^b	τ^c, ns	τ_0/τ^b
Zn·TPP	599,645		1.7	
5	607,650	1.6	0.9	2.0
6	615,668	3.1	0.5	3.6
7	606,652	4.0	0.4	4.2

[a] Room temperature. [b] Φ_0 (0.04)[1a] and τ_0 are, respectively, the fluorescence quantum yield and lifetime of the corresponding zinc-porphyrin model. [c] Estimated error: ± 0.1 ns.

cation was detected in the 600−700 nm spectral region.[28] The final spectrum recorded at the end of the temporal window of the experiment (1000 ps) was practically superimposable to the triplet spectrum observed in the nanosecond experiments.

Electrochemistry. Cyclic voltammetry measurements on **5**−**7** were performed in CH_2Cl_2. The electrochemical behaviors of Zn·TPP and of **10** were studied in the same experimental conditions for comparison. For mechanistic reasons (see Discussion), attention was focused on the potential values for the first oxidation and reduction processes. The results are summarized in Table 7: the first oxidation process was assigned to the zinc-porphyrin unit, whereas the first reduction process can be easily attributed to the reduction of the bipy ligand on the rhenium unit.

(28) Kadish, K. M.; Shiue, L. R.; Rhodes, R. K.; Bottomley, L. A. *Inorg. Chem.* **1981**, *20*, 1274–1277.

Table 7. Electrochemical Data for **5**−**7**, and for the Reference Compounds Zn·TPP and [*fac*-Re(CO)$_3$(bipy)(py)][CF_3SO_3] (**10**)[a]

compound	$E_{1/2\ (red)}$[b] (V)	$E_{1/2\ (ox)}$[b] (V)	E^{0-0} (S_1) (eV)[c]	ΔG_{el} (eV)[d]
Zn·TPP	−1.38	+0.80		
10	−1.13	+1.74		
5	−1.16	+0.83	2.04	−0.05
6	−1.15[e]	+1.10	2.02	+ 0.23
7	−1.17	+0.83	2.05	−0.05

[a] All measurements were made in argon deaerated dichloromethane solutions at 298 K (0.1 M TBA(PF_6) as electrolyte, scan rate 200 mV/s, SCE as reference electrode, and glassy carbon as working electrode). [b] Half-wave potential in cyclic voltametry ($\Delta E_p = 60-80$ mV). [c] Estimated from the fluorescence spectrum. [d] Free energy change for intramolecular electron transfer from the excited (S_1) zinc-porphyrin unit to the bypiridine-rhenium unit. [e] Four-electron process.

Discussion

It is to be expected that the geometrical features of isomeric metal-mediated assemblies containing either 4′PyPs, or the corresponding 3′PyPs, are quite different. In 4′PyPs the geometry of the (pyridyl)N-metal bonds is easily predictable as they lay in the mean plane of the chromophore, regardless of the orientation of the *meso* pyridyl rings. On the contrary, in 3′PyPs the (pyridyl)N-metal bonds lay either above or below the porphyrin plane and their exact geometry is hardly predictable a priori.

According to X-ray data, 3′TPyP can adopt at least three different conformers in the solid state (Supporting Information). We showed in this work that the central 3′TPyP unit of compound **4** adopts, in the solid state, a 1,2-alternate conformation. The NMR spectra suggest that, in solution, **4** presents a number of different conformers in equilibrium at an intermediate-to-slow rate on the NMR time scale at room temperature. However, we previously described the molecular structure of the pentameric porphyrin assembly [{Ru(TPP)(CO)}$_4$(μ-3′TPyP)], in which the axially bound Ru(TPP)(CO) units lay alternatively above and below the plane of the central 3′TPyP (1,3-alternate conformer).[29] This conformation is imposed by obvious steric reasons and, consistent with the NMR data, is strictly maintained also in solution. There is only another example of a structurally characterized discrete assembly in which 3′TPyP is bound to four equal peripheral metal centers: the charged tridimensional prism [{Pd(en)}$_6$(μ-Zn·3′TPyP)$_3$](NO$_3$)$_{12}$ (en = ethylenediamine) described by Fujita and co-workers.[30] In this compound the three Zn·3′TPyP units have yet another conformation, in which all pyridyl rings have a *syn* orientation (*all-syn* conformer), with the connecting Pd fragments laying above the planes of adjacent porphyrins. Most likely this is the only conformer that allows formation of a cyclic species.

It is worth stressing that in the isomeric porphyrin-Re(I) compounds the relative geometry of the chromophore and of the Re(bipy) fragments depend remarkably on the position of the pyridyl N atom(s): in the 4′PyP compounds the planes of the porphyrin and of bipy are almost orthogonal, whereas in the 3′PyP derivatives, regardless of the conformation assumed by the porphyrin, they are canted and closer to one another (see Figure 7).

The supramolecular nature of the systems studied (as demonstrated by the additive nature of the spectroscopic and electrochemical properties of the molecular components,

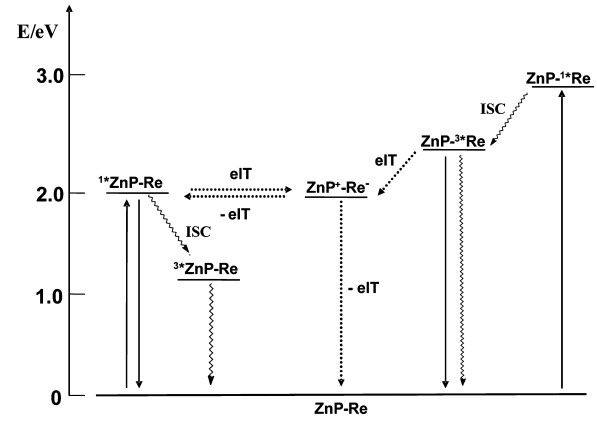

Figure 12. Energy level diagram for **5** in dichloromethane and photophysical processes.

Tables 5 and 7) allowed us to construct the energy level diagram as a superposition of those of the component units. To this simple picture, possible states of intercomponent charge-transfer character should be added. Given the well-known electron accepting properties of the [*fac*-Re(CO)$_3$(bipy)(py)]$^+$ unit,[10,16] a charge transfer state (Zn·porph$^+$-Re(bipy)$^-$), in which an electron is transferred from the zinc-porphyrin to the rhenium-bipy unit, is expected to lie close in energy to the singlet state (S_1) of the zinc-porphyrin unit. The energy of this state can be obtained as the difference in the potentials for oxidation of the Zn-porphyrin component and for reduction of Re(bipy) component.[31] The resulting energy diagram for the dimeric species is reported in Figure 12. The energy values inferred from electrochemical data (see Table 7) for the Zn·porph$^+$-Re(bipy)$^-$ charge transfer state are 1.99 and 2.25 eV for dimeric and pentameric species, respectively. It is worth noting that for **6** it lies significantly higher in energy with respect to the local S_1 state of the zinc-porphyrin ($E(S_1) = 2.02$ eV estimated from the fluorescence spectrum), whereas in the case of the dimeric species (**5** and **7**) it is practically isoenergetic with the S_1 state. Therefore, conversion from singlet porphyrin to the electron transfer state (eq 1) is clearly uphill ($\Delta G = 0.23$ eV, Table 6) for the pentanuclear compound **6**, and slightly allowed for the dimeric species ($\Delta G = -0.05$ eV).

$^{1}*Zn·porph-Re(bipy) → Zn·porph$^+$-Re(bipy)$^-$ (1)

The photophysics was studied by excitation at $\lambda > 500$ nm where the light is absorbed selectively by the zinc-porphyrin component. The most interesting observation is that, in all the systems studied, the typical fluorescence of the zinc-porphyrin unit is reduced in intensity and lifetime by the presence of the peripheral rhenium-bipy fragment(s) (Table 6). The differences with respect to the model **10** are not large but clearly outside the experimental error. As far as potential quenching mechanism is concerned, two possibilities should be considered: (i) electron transfer quenching and (ii) heavy-atom effect.

(29) Alessio, E.; Geremia, S.; Mestroni, S.; Srnova, I.; Slouf, M.; Gianferrara, T.; Prodi, A. *Inorg. Chem.* **1999**, *38*, 2527–2529.
(30) Fujita, N.; Birhadha, K.; Fujita, M.; Sakamoto, S.; Yamaguchi, K. *Angew. Chem., Int. Ed.* **2001**, *40*, 1718–1721.

Transient spectroscopy is a useful tool to investigate the quenching mechanism. Nanosecond time-resolved spectroscopy of the Zn·porphyrin-Re(I) dyads showed that the electron transfer quenching is relatively inefficient. Support for this conclusion comes also from the ultrafast absorption experiments where no evidence for formation of the charge transfer product was observed. Evidently, in the present systems, the driving force for the electron transfer (eq 1) is too small so that the process is not fast enough to compete with the intersystem crossing in the porphyrin unit. Given the strong spin−orbit coupling of the rhenium atom, the most likely explanation for the fluorescence quenching in these systems is the spin−orbit perturbation (heavy atom effect), that is, the enhancement by spin−orbit coupling of a formally spin-forbidden deactivation process of the singlet state of the porphyrin. In the free-base compounds **1** and **2**, where photoinduced electron transfer from excited porphyrin to rhenium unit is thermodynamically forbidden, we concluded that fluorescence quenching occurs through the heavy atom effect.[16] As discussed in our previous works,[1,16,32] this effect is a general feature for porphyrin arrays containing peripheral heavy atoms and its magnitude correlates with the number of metal centers connected to the porphyrin core. The observations that also in the present systems the fluorescence quenching is more efficient for pentameric with respect dimeric species, and that it is not affected by the solvent polarity, provide additional evidence for an heavy metal quenching mechanism.[33]

The quenching efficiency is substantially higher for the dyad **7** than for the isomeric dyad **5** (Table 6). Given that the Re(bipy) fragment is closer to the porphyrin in **7** than in **5**, this result suggests an effect of the distance on the heavy atom-induced quenching.[34]

Recently Perutz and co-workers reported an interesting and detailed photophysical study of the dyad [*fac*-Re(CO)$_3$(3-pic)(bipy-Zn·porph)]$^+$ (**11**, see Introduction and Figure 2) where two molecular units very similar to those of our systems, a zinc-tetraphenylporphyrin and a rhenium(I)-bipy complex, are covalently linked via an amide bond.[13,14] A complete quenching of the porphyrin fluorescence was observed, together with a drastic shortening of the singlet porphyrin lifetime (24 ps measured in nitrile solvents by time-resolved absorption experiments in the visible). In addition, an ultrafast photoinduced electron transfer process from the Zn·porphyrin to the Re(I)-bipy unit was revealed by time-resolved infrared spectroscopy.[14]

Despite the similarity of the molecular component units (see Figures 1 and 2), the dyads **5** and **7** studied in the present work differ from **11** for the absence of photoinduced electron transfer. The reasons for this different behavior can be analyzed in terms of standard electron transfer theory. In the limit of weak-interaction (nonadiabatic regime), the rate constant for an electron transfer process is given by eq 2:

$$k = \frac{2\pi}{\hbar} H_{DA}^2 FCWD \qquad (2)$$

where H_{DA} is the electronic coupling between donor and acceptor and *FCWD* is the nuclear term (Franck−Condon weighted density of states) that accounts for the combined effects of the reorganizational energies and driving force. For **11** photoinduced electron transfer ($\Delta G = -0.24$ eV) is substantially more exergonic than for **5** and **7** (Table 7). Thus, as the processes fall in the activated region, electron transfer is predicted to be much faster for **11**. As far as the electronic factor is concerned, it is important to stress that the two types of systems differ in the connection of the two molecular components. At first sight, a better electronic factor could be expected for our systems, where the porphyrin unit is directly coordinated to the rhenium complex via the pyridyl group, whereas an amido bridge is interposed in **11**. However, in **11** the connection takes place at the bipy ligand, that is, at the site involved in the reduction, whereas in the dyads **5** and **7** bipy is an ancillary ligand of rhenium center. Thus, the effects of the structural differences on the electronic factor are difficult to predict.

We found that, for **5** and **7**, addition of pyridine causes significant increase of the fluorescence quenching, shortening the lifetime from 900 to ca. 250 ps. More interestingly, the biphasic behavior observed by ultrafast spectroscopy experiments (the initial spectrum, taken immediately after the excitation pulse, evolved to a final spectrum through the formation of an intermediate state, Figure 11) is consistent with a picture in which the charge separated state (Zn·porph$^+$-Re(bipy)$^-$) is sufficiently close in energy to the singlet state (S_1) to allow a fast equilibration between them. Thus, in the presence of pyridine: (i) first, an electron transfer process from the singlet of the zinc-porphyrin to the Re(bipy) fragment takes place with a time constant of 20 ps, leading to the charge separated state; (ii) second, the equilibrium mixture of singlet and charge separated states decays to the triplet state in 300 ps. This value is in good agreement with the lifetime measured in the emission experiment (250 ps). The absence of the absorption features of the charge separated state in the transient spectrum may be attributed to concomitant causes: (i) at equilibrium the population of the charge transfer state could be relatively small; (ii) it is difficult to distinguish the spectrum of the porphyrin radical cation from that of the S_1 and T_1 excited states because they are very similar in the 450−650 region.[14,28]

Similar results were reported by Gust et al. who observed a drastic increase of the rate of intramolecular electron-transfer quenching in a zinc/free-base bis-porphyrin system upon addition of pyridine in CH_2Cl_2. They found that the axial coordination of pyridine to zinc lowers the oxidation potential of the zinc-porphyrin with consequent stabilization of the interporphyrin charge transfer state and increase of the driving force for electron-transfer.[26] The same conclu-

(31) No correction for electrostatic work terms is required in this case because of the charge shift character of the process involved.
(32) (a) Prodi, A.; Indelli, M. T.; Kleverlaan, C. J.; Scandola, F.; Alessio, E.; Gianferrara, T.; Marzilli, L. G. *Chem. Eur. J.* **1999**, *5*, 2668–2679. (b) Alessio, E.; Geremia, S.; Mestroni, S.; Iengo, E.; Srnova, I.; Slouf, M. *Inorg. Chem.* **1999**, *38*, 869–875.
(33) Remarkably, the increase of the extent of quenching ($\tau°/\tau$) with increasing the number of rhenium centers from one to four (see Table 6) is the same as that observed for the corresponding free base adducts (see ref16).
(34) Abegg, P. W.; Ha, T.-K. *Mol. Phys.* **1974**, *27*, 763–767.

sions can be drawn in our case: the stabilization of charge separated state ($Zn^{\bullet}porph^{+}$-Re(bipy)$^{-}$) caused by the presence of pyridine leads to an increase of the rate constant for the electron transfer that becomes competitive with the intersystem crossing for the deactivation of the singlet state.

Conclusions

The Re(I)-dmso complex [*fac*-Re(CO)$_3$(bipy)(dmso-O)]-(CF_3SO_3) (**9**) proved to be an excellent precursor for the facile attachment of the [*fac*-Re(CO)$_3$(bipy)]$^+$ fragment to pyridylporphyrins. In the literature there are several examples of 4′PyPs bound to metal fragments,[1−5] but those with 3′PyPs are much less abundant. This work confirmed that the geometrical features of 3′PyPs conjugated to multiple metal fragments are hardly predictable and that in solution conformational equilibria occur, provided that the peripheral complexes have a moderate steric bulk.

Even though in the adducts described in this work the porphyrin-Re(I) connection relies on a single bond, they proved to be extremely stable in solution and no dissociation of the porphyrin was observed, even in the presence of a large excess of a competitor ligand such as pyridine. Thus, from this point of view, the Re(I)-PyPs adducts compare well with the alternative compounds in which the porphyrin is connected to Re(I) through a chelating bipy unit.[13,14]

This study shows that, upon insertion of Zn into the porphyrin core, the photophysical behavior of the adducts changes appreciably compared to the free-base analogues.[16] In particular, in the dyads **5** and **7** the charge separated state $Zn^{\bullet}porph^{+}$-Re(bipy)$^{-}$ decreases in energy so that it becomes almost isoenergetic with the excited singlet of the zinc-porphyrin unit. We had no evidence for electron transfer quenching in the dyads as such, whereas the addition of pyridine (that binds axially to zinc) led to a moderately efficient photoinduced electron transfer process. We can conclude that our dyads have a borderline energetic situation in which slight modifications in the porphyrin chromophore and/or in the coordination sphere of the Re(I)-bipy fragment may increase the energy difference between the two states and, as a consequence, the efficiency of the photoinduced electron transfer process. In perspective, both fragments can be separately fine-tuned through an appropriate functionalization of the bipy ligand and/or of the *meso* phenyl rings of the porphyrin and then connected through the facile synthetic procedure described above. This approach will lead to new conjugates that might be suited for being tested in photocatalytic reactions. Ongoing work toward this direction is underway in our laboratory.

We were also interested to assess how the photophysics of these systems is affected by the number of Re(I) fragments and by their relative positions with respect to the porphyrin chromophore. This work showed that an increase in the number of peripheral pyridyl rings (i.e., going from mono- to tetrapyridylporphyrin) is detrimental in that it leads to an increase in the energy of the charge-separated state. In addition, the increased number of Re atoms leads to a more efficient quencing of the porphyrin fluorescence by heavy-atom effect.

Finally, even though in the $Zn^{\bullet}porph$-Re(bipy) dyads the energetic for the electron-transfer process is not affected by the geometry of the porphyrin, the heavy-atom induced fluorescence quenching is substantially more efficient for the 3′MPyP than for the 4′MPyP dyad, that is, it depends on the distance between the two fragments. This result suggests that future work should be focused on 4′PyPs-Re(I) conjugates.

Acknowledgment. We thank C. Chiorboli for the ultrafast spectroscopy measurements. This work was supported by the Italian Ministry for University and Research, project FIRB-RBNE019H9K. The CNR staff at ELETTRA (Trieste) are acknowledged for help in the use of the facility supported by CNR and by Elettra Scientific Division.

Supporting Information Available: Crystal packings of **1** and **3**; ^{1}H NMR spectra of **1**, **2**, **4**, **5**, **6**, **7** (effect of the addition of CD_3OD), and **8**; transient absorption spectra upon laser flash photolysis of **5** and of the reference $Zn^{\bullet}$TPP chromophore; schematic drawings of the three possible limit conformers of 3′TPyP; X-ray crystallographic data in CIF format for the structures reported in this paper. This material is available free of charge via the Internet at http://pubs.acs.org.

IC800971E